Published in final edited form as:
ChemMedChem. 2010 November 8; 5(11): 1871–1879. doi:10.1002/cmdc.201000222.

Active Core in a Triazole Peptide Dual Site Antagonist of HIV-1 gp120

Dr. Muddegowda Umashankara,
Department of Biochemistry and Molecular Biology, Drexel University College of Medicine, Philadelphia, Pennsylvania 19102 (USA)

Karyn McFadden,
Department of Biochemistry and Molecular Biology, Drexel University College of Medicine, Philadelphia, Pennsylvania 19102 (USA)

Isaac Zentner,
Department of Biochemistry and Molecular Biology, Drexel University College of Medicine, Philadelphia, Pennsylvania 19102 (USA)

Dr. Arne Schön,
Department of Biology, The Johns Hopkins University, Baltimore, Maryland 21218 (USA)

Dr. Srivats Rajagopal,
Department of Biochemistry and Molecular Biology, Drexel University College of Medicine, Philadelphia, Pennsylvania 19102 (USA)

Ferit Tuzer,
Department of Biochemistry and Molecular Biology, Drexel University College of Medicine, Philadelphia, Pennsylvania 19102 (USA)

Syna A Kuriakose,
Department of Biochemistry and Molecular Biology, Drexel University College of Medicine, Philadelphia, Pennsylvania 19102 (USA)

Dr. Mark Contarino,
Department of Biochemistry and Molecular Biology, Drexel University College of Medicine, Philadelphia, Pennsylvania 19102 (USA)

Dr. Judith LaLonde,
Department of Chemistry, Bryn Mawr College, Bryn Mawr, PA 19010 (USA)

Prof. Ernesto Freire, and
Department of Biology, The Johns Hopkins University, Baltimore, Maryland 21218 (USA)

Prof. Irwin Chaiken*
Department of Biochemistry and Molecular Biology, Drexel University College of Medicine, Philadelphia, Pennsylvania 19102 (USA)

Abstract

In an effort to identify broadly active inhibitors of HIV-1 entry into host cells, we had previously reported a family of dodecamer triazole-peptide conjugates with nanomolar affinity for viral

Fax: 215-762-4452, ichaiken@drexelmed.edu.

Supporting Information **Available**
I. MALDI-TOF spectrometry and RP-HPLC analytical chromatograms for all reported peptides.
II. ELISA competition assays, antiviral assays, and SPR sensorgrams for all reported peptides.

surface protein gp120. This class of peptides exhibits potent antiviral activity and the capacity to simultaneously inhibit interaction of viral envelope protein with both CD4 and co-receptor. In the current investigation, we used minimization of structural complexity of the lead triazole inhibitor HNG-156 (peptide **1**) in order to explore the limits of the pharmacophore that enables dual antagonism and to improve opportunities for peptidomimetic design. Truncations of both carboxyl- and amino-terminal residues of the initial 12 amino acid residues of peptide **1** were found to have minimal effect on both affinity and antiviral activity. In contrast, the central triazole Pro-Trp cluster at residues 6 and 7 with ferrocenyl-triazole-Pro (Ftp) was found to be critical for bioactivity. Amino terminal residues distal to the central triazole Pro-Trp sequence tolerated decreasing degrees of side chain variation upon approaching the central cluster. A peptide fragment containing residues 3-7 (Asn-Asn-Ile-Ftp-Trp) exhibited substantial direct binding affinity, antiviral potency, dual receptor site antagonism and induction of gp120 structuring, all properties defining the functional signature of the parent compound **1**. This active core contains a stereochemically specific hydrophobic triazole-Pro-Trp cluster, with a short N-terminal peptide extension providing groups for potential main chain and side chain hydrogen binding. The results of this work argue that the pharmacophore for dual antagonism is structurally limited, enhancing the potential to develop minimized peptidomimetic HIV-1 entry inhibitors that simultaneously suppress binding of envelope protein to both of its host cell receptors. The results also argue that the target epitope on gp120 is relatively small, pointing to a localized allosteric inhibition site in the HIV-1 envelope that could be targeted for small-molecule inhibitor discovery.

Keywords

HIV-1; surface plasmon resonance; entry inhibitors; click chemistry; peptide triazole

Introduction

Human immunodeficiency virus-1 (HIV-1) is the etiological agent of acquired immunodeficiency syndrome (AIDS).[1] As of 2009 the virus had infected 33.4 million people worldwide, with 2.7 million new infections each year leading to the persistence of the global AIDS pandemic.[2] HIV-1 entry is mediated by the viral envelope glycoprotein spike, which is derived from the proteolytic cleavage of gp160 into gp120 and gp41 subunits.[3] The first step in productive viral entry into the host cell involves the high-affinity attachment of gp120 to the N-terminal domain of CD4.[4] This binding interaction initiates conformational changes in gp120 that stabilize a binding domain for subsequent interaction with a host cell chemokine receptor (often denoted ‘co-receptor’, most frequently CCR5 or CXCR4).[5] Co-receptor binding allows for further envelope/receptor rearrangement that leads to fusion of virus and cellular membranes and delivery of viral replication proteins and RNA into the cells.[6]

The proteins involved in the entry process, on both the host cell and the virus, provide multiple targets for functional intervention.[7] Fusion inhibitors have begun to emerge as a promising new class of HIV therapeutics, by blocking conformational changes within gp41.[8] In addition, several small molecules[9] and peptidomimetics[10] have been reported that compete directly for CD4 binding to its binding pocket in gp120. CD4 mimetics have the benefit of targeting the most conserved binding site identified so far in the gp120 protein, with the caveat that these molecules often induce conformational changes that can lead to enhanced co-receptor binding. It has recently been shown, however, that the activated state of the gp120/gp41 complex caused by the binding of CD4 and CD4 mimetics is short-lived and is followed by complete loss of function of the virion.[11]

Novel agents that can simultaneously inhibit both gp120-CD4 and gp120-co-receptor interactions have substantial benefit for developing entry inhibitor drugs. We have previously reported a family of peptide conjugates that exhibit high affinity binding to gp120 and inhibit interactions of gp120 with both CD4 and the co-receptor surrogate mAb 17b.[12] These peptides were generated by click chemistry with alkynes[13] on an azidoproline at position 6 of the parent 12mer peptide (12p1, RINNIPWSEAMM).[14] Structure-activity relationship analysis led to identification of **1**, the ferrocene triazole conjugated peptide HNG-156,[15] which has low nM affinity for HIV-1 gp120 and strong potency for inhibiting cell infection. In the present study, we investigated whether smaller active fragments of **1** could be formed by truncating both the C- and N-terminal regions of **1**, as well as by specific residue replacements, in order to explore a pharmacophore core which could lead to the design of smaller peptidomimetic inhibitors. Through this work, active fragments were found to have substantial binding and antiviral activity, retained the dual receptor site antagonism signature of the 12-residue starting compound and have structure-inducing effects on gp120 consistent with stabilization of a conformationally inactivated Env protein state. This indicates the presence of a localized allosteric inhibition site in gp120 and the potential to target this site with structure-minimized peptidomimetic ligands in the search for entry inhibitor leads.

Results

Retention of function of an N-terminal fragment containing the central triazole (Pro)-Trp cluster

The high affinity and antiviral potency of the 12mer metallocene-conjugated peptide HNG-156 (Peptide **1**, Table 1) led us to the current work aimed at identifying sequence-minimized peptides that retain the dual antagonist inhibition function characteristic of **1**. The essential triazole-indole side chain cluster in the middle of the peptide provided a focal point for initial truncation analysis. We truncated parent full-length peptide **1** into C and N-terminal heptapeptides **2** (residues 6-12) and **3** (residues 1-7), such that both truncated peptides retained the central triazole-indole moiety. The two truncates were compared for their ability to bind gp120 using SPR. Increasing concentrations of **2** and **3** were passed separately over a high-density (3500 RU) HIV-1_{YU-2} gp120 surface. The binding data were fit to a bimolecular binding process. The N-terminal fragment peptide **3** binds to gp120 (K_D = 12.9 nM) with comparable affinity to **1** while the C-terminal fragment peptide **2** binds to gp120 with 809 nM K_D, which is 100 fold lower affinity versus the 12mer peptide (Figure 1A, B; Table 2).

Since the parent peptide **1** has been found to inhibit gp120 interactions at both its CD4 and co-receptor binding sites, we examined the inhibition of HIV-1_{YU-2} gp120 interactions with immobilized sCD4 and mAb 17b by fragment peptides **2** and **3** using both ELISA and SPR analysis. As shown in Figure 1B and C, peptide **3** maintained the dual antagonist signature. Mean inhibitory concentration (IC_{50}) for **3** by SPR was 500 nM and 250 nM for sCD4 and mAb 17b, respectively (Table 2). Peptide **2** was unable to inhibit either sCD4 or mAb 17b binding to gp120 at concentrations up to 10 μM, in contrast to its detectable binding to gp120. In control experiments, neither **2** nor **3** exhibited direct binding to either a sCD4 or mAb 17b SPR chip surface (data not shown).

We examined the antiviral activities of **2** and **3** using single round infection of target cells by HIV-1_{BaL}. The antiviral potency of **3** is only slightly diminished compared to the parent peptide **1**, consistent with the direct binding data. The C-terminal peptide **2** had a significant reduction in potency with an IC_{50} value of 35 μM as compared to 0.8 μM for **1** (Figure 2, Table 2). Neither of these compounds inhibited negative control viruses pseudotyped with

the VSV-G envelope (data not shown), indicating that the inhibition is specific to the HIV-1 envelope glycoprotein.

To assess the importance of Ser 7 in the C-terminal region of **1**, we evaluated the binding and dual antagonist property of peptide **4**, in which the additional serine residue was present at the C-terminus. Incorporation of this Ser led to a relatively small and variable effect on the direct binding and antiviral properties versus those for peptide **3** (Table 2) arguing against a major role for this residue.

Progressive truncation and sequence variation of the N-terminal residues to identify minimum length active dual antagonist sequences

To assess the functional importance of N-terminal amino acids, we first examined the significance of Arg residue 1 for direct binding to gp120 and antiviral activity of peptide **4** by replacing this positively charged residue with the negatively charged residue Glu. The resulting peptide **5** enhances the direct binding affinity for gp120 (K_D = 5.5 nM), as well as antiviral potency (IC_{50}=1.2 μM) (Table 2). Although peptide **5** showed somewhat increased efficacy versus **4**, both Arg and Glu at position 1 were acceptable. These findings argue that the positively charged side chain of Arg residue at the N-terminus is relatively unimportant.

In peptide **6**, we truncated the N-terminus further to remove the Arg residue and found that this deletion only partially reduced the direct binding activity (K_D = 169 nM), mainly due to increased off-rate of the peptide in SPR analysis (Figure 3B). In addition, peptide **6** retained significant antiviral potency in single round infection assays. We went on to evaluate side chain variations with different functionalities of the N-terminal Ile residue in peptide **6**. A series of hepta-peptides (**Y-Asn-Asn-Ile-X-Trp-Ser**), where Y=Arginine (**7**), Glutamic acid (**8**), Citrulline (**9**), Lysine (**10**) and Phenylalanine (**11**) and X = ferrocene conjugated triazolePro, were evaluated for their direct binding and inhibition of viral infection activities. In general, these replacements led to peptide fragments with similar antiviral potencies and binding activities (Table 2). Interestingly, replacement with the unnatural amino acid citrulline in **9** significantly increased the direct binding affinity to K_D = 4.1 nM (Figure 3C) and antiviral potency to IC_{50} = 2.6 μM (Table 2). Variation of amino acid side chain does not affect either the direct binding or antiviral potency of the 7mer peptide, indicating that specific interaction of the side chain of the amino acid in the Ile position with gp120 is not essential for the viral inhibition function. This was further supported by the substantial, though somewhat reduced, activities observed with the hexa-peptide **12**, in which the Ile residue of peptide **6** was truncated.

In contrast to the relatively small effects from sequence replacements at N-terminal residues of 1 and 2 in the parent peptide **1**, the Asn residue in position 3 is substantially more sensitive. We investigated replacement of the Asn residue in peptide **12** with Arg (**13**), Glu (**14**), Cit (**15**) and Ile (**16**) by ELISA, SPR and antiviral assays. Side chain variations of Asn in position 3 led to substantial suppression of antiviral activity and direct binding affinity to gp120 (Table 2). This suggests that the Asn side chain at position 3 is important for function. This conclusion is further supported by the complete loss of activity of penta-peptide **20**, which was derived from the N-terminal truncation of the Asn residue in peptide **12**.

Active core sequence within the peptide triazole inhibitors

Based on the above findings that several residues in the N- and C-terminal regions had limited importance for gp120 binding and inhibition, we explored the limits of truncation. Deletion of the C-terminal Trp residue led to complete loss of activity in **18**. In contrast, two fragments, **17** and **12**, were found to retain substantial binding, dual site antagonism and

antiviral activity (Table 2). We tested the five-residue peptide **19**, containing residues 3-7 of parent peptide **1.** This peptide was found by SPR to bind to gp120 with weakened though still finite affinity with K_D = 333 nM (Figure 3D) and exhibited significant antiviral activity (IC_{50} = 33 μM). An alternative penta-peptide **20**, containing residues 4-8, was found to be inactive.

In addition to its dual antagonism of CD4 and mAb 17b binding, the core peptide **19** was found to suppress the interaction with other ligands of gp120 that are dependent on the conformation of the Env protein. Previous work [15] showed that compound **1** inhibited binding to monoclonal antibodies mAb b12 and mAb F105 to the viral glycoprotein gp120. ELISA data presented in Figure 4 show that the active pharmacophore pentapeptide **19** retains similar functionalities.

Importance of stereochemistry in the triazolePro-Trp cluster

The active core sequences found in this work embody a C-terminal hydrophobic cluster. Previous work has shown that the stereochemistry of the triazolePro residue in this cluster in compound **1** was critical, in that the *S* configuration of triazole was active while *R* configuration was not.[13] Here, we examined the stereochemical requirements in the Trp position of the cluster. Compared to **9** (all-L amino acids), **21** with D-Trp substituted was virtually inactive (Table 2). Taking these new and previous observations together, it is clear that the function of peptide triazole inhibitors is highly dependent on the stereochemistry of the “triazolePro-Trp” cluster.

Preservation of conformational effects on gp120 by truncated peptide triazoles

Prior ITC analysis with analogues of compound **1** showed that binding of the parent peptide triazole had the ability to structurally constrain gp120.[13] The change in conformation induced upon binding would explain the ability of the peptide to inhibit both CD4 and coreceptor binding. Here, we examined whether the property of conformational structuring was retained in the peptide triazole truncates. The results of Figure 5 compare the calorimetric titration data for parent peptide **1** with those for truncated peptides **9**, **19** and **20**. The thermodynamic parameters obtained by ITC for these and other peptides are summarized in Table 3. Except for the low affinity peptide **20**, all of the peptide truncates tested were similar to compound **1** in showing large favorable enthalpy and unfavorable entropy changes. CD4 binding to gp120 is also characterized by a large change in favorable enthalpy ($\Delta H = -34.5$ kcal mol^{-1}) that is coupled to a large unfavorable change in entropy ($\Delta S = -79$ cal K^{-1} mol^{-1}; $-T\Delta S = 23.6$ kcal mol^{-1}) that together with a large negative heat capacity change ($\Delta C_p = -1800$ cal K^{-1} mol^{-1}) make up the thermodynamic signature for a binding event that is associated with a large conformational structuring of gp120[9c,16] Although the thermodynamic changes are much larger for CD4 binding to gp120, some conformational structuring is likely to be induced also upon binding of the peptides truncates presented here.

Discussion

In this work, we explored structural minimization of a peptide triazole class of potent HIV-1 entry inhibitor candidates. The starting point was the 12-residue peptide **1**, which has a low nanomolar affinity for Env protein, can inhibit the binding of Env gp120 to both CD4 and co-receptor binding sites and neutralizes HIV-1 infection. Through examination of a range of chemically synthesized peptide derivatives, we found that truncated fragments of **1** retained significant binding and inhibition activities. Truncations at the C-terminal residues were most tolerated, while those for the first two N-terminal residues Arg and Ile were largely tolerated. The internal sequence cluster of X-Trp, in which X was the

ferrocenyltriazole on Pro at position 6 of **1**, was required for function. Amino-terminal extensions of 3 residues from this cluster provided a minimized functional core. The shortest sequences observed so far with the dual antagonist signature, namely compounds **12, 17** and **19**, retained substantial antiviral and binding activities.

The ability to produce size-minimized fragments that retain potent antiviral activity argues for the potential to derive smaller inhibitors by focusing on the crucial triazolePro-Trp cluster and short N-terminal extensions from this cluster. The presence of a hydrophobic cluster infers the importance of interactions of its hydrophobic side chains with complementary epitopes in Env protein, with the N-terminal extension providing other types of stabilizing contacts with the protein. The stereochemical nature of the triazolePro-Trp clearly is critical. Previous work has shown that greater activity of peptides is obtained with the *S* configuration versus *R* in the triazole side chain.[13] The current study shows that switching the main chain configuration at Trp from L to D also leads to a large decrease of inhibitory function. Likely, the specific stereochemistry provides an arrangement of structural elements in the triazolePro-Trp cluster enabling productive complementary contacts with gp120. While we cannot define from current data what the arrangement of structural elements are at the peptide triazole-gp120 interface, one may speculate that both peptide-protein contacts and intra-peptide interactions can occur. In any case, we may conclude that the triazolePro-Trp sequence provides a spatially-arranged aromatic cluster, while the N-terminal extension of residues may make hydrogen bonding interactions that help stabilize productive Env protein binding. The sequence starting point of greatly shortened peptides, such as **12**, **17** and **19**, implies the potential to form smaller peptidomimetic compounds that retain the essential structural elements embodied in the minimized peptides.

The observation in the current work of active core peptide fragments implies that the target site for inhibition is substantially localized within the gp120 protein. Twelve residue peptides such as **1**, especially in an elongated conformation, have at least the potential to bind to a relatively large surface area of gp120, leaving open exactly how large and well-defined the inhibitor binding site could be. In contrast, observing functionality in much smaller fragments makes it more likely that the inhibitor binding site of Env gp120 involves a relatively small footprint on the Env surface. That the putative allosteric site of the HNG/UM classes of inhibitors exhibits strong stereo-specificity of the small hydrophobic triazolePro-Trp cluster further argues that this site can be a viable target for small molecule inhibitors. This suggests the potential to screen for small molecule HIV-1 entry inhibitor leads that block HNG/UM peptide binding, exhibit dual antagonist activity and retain antiviral activity.

Experimental section

Reagents

The following reagents were obtained from the NIH AIDS Reference and Reagent Program, Division of AIDS, NIAID: HIV-1 gp120 Monoclonal Antibody (b12) from Dr. Dennis Burton and Dr. Carlos Barbas; HOS.CD4.CCR5 cells and pNL4-3.Luc. R-E- from Dr. Nathaniel Landau; pHEF-VSV-G from Dr. Lung-Ji Chang; CHO-ST4.2 cells from Dr. Dan Littman; Monoclonal Antibody 17b was obtained from Strategic Biosolutions. The plasmid for monomeric HIV-1_{YU-2} gp120 was a generous gift from Dr. Joseph Sodroski. The plasmid for HIV-1_{BaL} gp160 was a generous gift from Dr. Julio Martin-Garcia.

Peptide Synthesis and Purification

The sequences and denotations of all peptides reported are given in Table 1. Peptides were synthesized manually by stepwise solid-phase peptide synthesis on a Rink Amide Resin with

a substitution value of 0.7mmole gm^{-1} (Novabiochem). All Fmoc-amino acid derivatives and coupling reagents were purchased from Chem-Impex International, Inc. Synthesis grade solvents were used in all procedures. *9*-Fluorenylmethoxycarbonyl (Fmoc) group was employed for protection of the α-amino group during coupling steps. Side chain protecting groups were triphenylmethyl (Trt) for Asn, tert-butyl (tBu) for Ser and tert-butyloxycarbonyl (Boc) for Trp. Coupling of each residue was carried out using HBTU/HOBt in Dimethylformamide (DMF). Four equivalents of each Fmoc protected amino acid were used for coupling. Cleavage of the peptide from the resin was performed using a cleavage cocktail comprising 90:2.5:2.5:5(v/v) trifluoroaceticacid (TFA)/thioanisole/ethanedithiol/H_2O at room temperature for 2 hours. After the filtration and washing of resin by TFA, excess of solvent was removed under vacuum. Crude peptides were treated with ice-cold diethyl ether and then centrifuged at 3000 rpm for 10 minutes at 4 °C. Synthetic peptides were purified by HPLC (Beckman Coulter System Gold) using a semiPrep Vydac C-18 column with a 5 to 60% acetonitrile/water (0.1% TFA) gradient over 75 minutes at 3 mL min^{-1} flow rate. All peptides were purified to ≥ 98% homogeneity as judged by analytical reverse phase HPLC on C-18. The integrity of purified peptides was confirmed by MALDI-TOF spectra. Analytical chromatograms and mass spectra for all peptides reported are given in the Supporting Material.

Protein Production

CHO-ST4.2 cells, which secrete the full extracellular domain of the CD4 protein (soluble CD4, sCD4), were grown in a hollow fiber bioreactor (FiberCell Systems, Inc.) in HiQ CDM4CHO media (Hyclone) supplemented with 4 mM L-glutamine, 300 nM methotrexate and 1% antibiotic/antimycotic. Supernatant was purified over a sulfopropyl-substituted ion exchange column (GE Healthcare) on an AKTA Fast Liquid Chromatography (FPLC) machine (GE Healthcare). Fractions were collected using a gradient buffer system consisting of 50 mM MES/50 mM NaCl and 50 mM MES/500 mM NaCl at pH 6.0. Fractions were dialyzed into 50 mM bis-tris propane at pH 6.0 and loaded onto a quaternary ammonium-substituted ion exchange column (GE Healthcare) using a gradient buffer system consisting of 50 mM bis-tris propane and 50 mM bis-tris propane/1 M NaCl at pH 9.0. The column flow-through containing purified CD4 was pooled and dialyzed into 1× PBS, pH 7.4 overnight at 4 °C. The CD4 protein was then concentrated using a 10 kDa Amicon centrifugal filter unit (Fisher Scientific). All proteins were analyzed by SDS-PAGE/coomassie stain (Invitrogen) and found to be of greater than 95% purity.

Full length HIV-1_{YU-2} gp120 with a C-terminal hexa-histidine epitope tag was produced by transient transfection of 293F cells according to manufacturer's protocol (Invitrogen). Cells were harvested, spun down and the supernatant filtered using 0.2 μm filters. Supernatant was purified over an F105-antibody coupled NHS-activated Sepharose column according to the manufacturer's instructions (GE Healthcare). HIV-1_{YU-2} gp120 was eluted from the column with 100 mM glycine buffer, pH 2.4. The samples were neutralized with 1:10 v/v addition of 1M Tris, pH 8.0 buffer immediately after elution. Peak fractions were collected and analyzed by SDS-PAGE. Single band fractions corresponding to the correct protein size were collected and concentrated, dialyzed against PBS and stored at −80 °C.

Preparation of Recombinant Luciferase Expressing Virus and Cell Infection Assays

Single round recombinant, luciferase-reporter viruses were produced in a HEK293T cells using Fugene transfection reagent (Qiagen) according to the manufacturer's protocol. Cells were seeded in T75 flasks (approximately 3×10^6 cells per flask) and transfected the following day with 4 μg of plasmid encoding the envelope (HIV-1_{BaL} or VSV-G) together with 8 μg of the envelope-deficient pNL4-3-Fluc+env− provirus developed by N. Landau. [17] Culture supernatants containing viral particles were collected 48-72 hours after

transfection, clarified by centrifugation, filtered, aliquoted and stored at -80 °C until use. For inhibition experiments, the viral stocks were first incubated with serial dilutions of the inhibitor at 37 °C for 30 minutes. The mixture was added to human osteosarcoma cells that stably express CD4 and CCR5 (HOS.CD4.CCR5) for 48 hours. The cells were then lysed with passive lysis buffer (Promega) followed by freeze-thaw cycles. Luciferase assays were performed using 1 mM D-luciferin salt (Anaspec) as substrate and detected on a 1450 Microbeta Liquid Scintillation and Luminescence Counter (Wallac and Jet). IC_{50} values were estimated using non-linear regression analysis with Origin V.8.1 (Origin Lab). All experiments were performed at least in triplicate and results were expressed as relative infection with respect to cell infected with virus in the absence of inhibitor (100% infected).

Competition ELISA

The ability of peptides to inhibit the binding of sCD4, mAb F105, mAb b12 and mAb 17b to gp120 was screened by competition ELISA. 100 ng HIV-1_{YU-2} gp120 was adsorbed to a 96-well microtiter plate overnight at 4 °C. After washing the plate three times with PBST buffer (1× PBS with 0.1% Tween-20 v/v), the plate was blocked with 3% BSA in 1× PBS for 2 hours at 25 °C, followed by washing of the plate 3 times with PBST. For the CD4 competition experiments, 100 μL of sCD4 (0.1 μg ml^{-1}) was added to each well in the presence of increasing concentrations of peptide (0.01, 0.02, 0.04, 0.08, 0.16, ----100 μM). This and all subsequent incubation steps until detection were done in 0.5% BSA in PBS. After 1hr incubation, the plate was washed 3 times with PBST followed by addition of 100 μL/well of biotinylated anti-CD4 antibody (eBioscience) at a 1:5000 dilution and the plate incubated for 1hr at 25 °C. After washing the plate, streptavidin-bound HRP (AnaSpec) was added at a 1:5000 dilution and again incubated for 1 hour at room temperature. To determine effectiveness of peptides to inhibit antibody binding to gp120, 100 μL of mAb 17b, mAb F105 and mAb b12 (0.1 μg ml^{-1} of each antibody) was added to the immobilized gp120 in the presence of increasing concentrations of peptide. After 1hr incubation at RT followed by washing three times, HRP-conjugated goat-antihuman antibody (CHEMICON) was added and incubated for 1 hour at RT. The extent of HRP conjugate binding was detected in both assays by adding 200 μL of *o*-phenylenediamine dihydrochloride (Sigma-Aldrich) reagent for 30 min followed by measuring optical density (OD) at 450 nm using a microplate reader (Molecular Devices).

Optical Biosensor Binding Assays

Surface plasmon resonance (SPR) interaction analyses were performed on a Biacore® 3000 optical biosensor (GE Healthcare). All experiments were carried out at 25 °C using standard 1× PBS, pH 7.4, with 0.005% Surfactant P-20. A CM5 sensor chip was derivatized by amine coupling by using *N*-ethyl-*N*-(3-dimethylaminopropyl)carbodiimide/*N*-hydroxy-succininide[18] with HIV-1_{YU-2} gp120 or, as a control surface, mAb 2E3 (monoclonal antibody to human Interleukin-5). For direct binding experiments, HIV-1_{YU-2} gp120 was immobilized on the sensor surface (~3500 RU); peptide analyte in PBS buffer (concentration range of 10 μM - 0.61 nM) was passed over the surface at a flow rate of 50 μl min^{-1} with a 5 minute association phase and a 5 minute dissociation phase. Regeneration of the surface was achieved by a single 5 second pulse of 10 mM glycine, pH 1.5. Analysis of peptide-mediated sCD4 and mAb 17b inhibition was achieved by injecting a fixed concentration of HIV-1_{YU-2} gp120 (100 nM), with increasing peptide concentrations, over sCD4 (~2000 RU) and mAb 17b (~900 RU) surfaces for 5 minute association and 5 minute dissociation at a flow rate of 50 μl min^{-1} in PBS. Regeneration of the surface was achieved by single 10 second pulse of 1.3 M NaCl / 35 mM NaOH and single 5-second pulse of 10 mM glycine, pH 1.5, for sCD4 and mAb 17b, respectively. All analyses were performed in triplicate.

SPR Data analyses were performed using BIAEvaluation 4.0 software (GE Healthcare). The responses of buffer injection and of signals observed in a control flow cell were subtracted to account for nonspecific binding. Experimental data were fitted to a simple 1:1 binding model with a parameter included for mass transport. The average kinetic parameters (association $\{k_a\}$ and dissociation $\{k_d\}$ rates) generated from a minimum of 3 data sets were used to define equilibrium dissociation (K_D) constants. The evaluation method for SPR inhibition data included a calculation of the inhibitor concentration at 50% of the maximal response (IC_{50}). The inhibition curve was converted into a calibration curve by the use of a fitting function. The fitting was done using the 4-parameter equation in BIAevaluation software:

$$Response = R_{high} - \frac{(R_{high} - R_{low})}{1 + \left(\frac{Conc}{A_1}\right)^{A_2}} \quad (1)$$

where $\mathbf{R_{high}}$ is the response value at high inhibitor concentrations and $\mathbf{R_{low}}$ is response at low inhibitor concentrations. **Conc** is the concentration of inhibitor, and $\mathbf{A_1}$ and $\mathbf{A_2}$ are fitting parameters. At the IC_{50} the following is true:

$$Response = R_{high} - \frac{(R_{high} - R_{low})}{2} \quad (2)$$

Under this condition, A_1 = Conc and is therefore taken as the desired IC_{50} parameter.

Isothermal Titration Calorimetry

Isothermal titration calorimetric experiments were performed using high-precision calorimetric systems of model VP-ITC or ITC_{20} (MicroCal Inc). The titrations described in this paper were performed by stepwise addition of peptide to gp120 contained in the calorimetric cell at a constant temperature of 25 °C. The VT-ITC has a cell volume of ~1.4 mL and the volume per injection of peptide is 10 μL, whereas ITC_{20} has a cell volume of ~200 μL and the peptide is injected in steps of 1.4 μL. For the experiments carried out in the VP-ITC the concentration of gp120 was ~2 μM and the syringe contained the peptide at a concentration of ~30 μM. For the experiment carried out using ITC_{20} gp120 was prepared at about 4 μM and the peptide at 50-100 μM. The solutions contained within the calorimetric cells and injector syringes were prepared in 1× PBS, pH 7.4 and thoroughly degassed to avoid bubble formation in the calorimetric cell. The heat evolved upon each injection of the peptide solution was obtained from the integral of the calorimetric signal. The heat associated with binding of a ligand to the protein in the cell was obtained by subtracting the heat of dilution from the heat of reaction. Heats of dilution due to mismatch between the syringe and cell solutions were negligible in all experiments. The individual heats were plotted as a function of the molar ratio, and nonlinear regression of the data provided the enthalpy change (ΔH) and the association constant ($K_A = K_D^{-1}$).

Supplementary Material

Refer to Web version on PubMed Central for supplementary material.

Acknowledgments

This research was supported by National Institute of Health grants P01 GM 56550 and R21 AI071965, as well as a grant from International Partnership for Microbicides/USAID. EF also acknowledges support from the National Institutes of Health GM 57144 and the National Science Foundation MCB 0641252.

References

1. a) Barre-Sinoussi F, Chermann JC, Rey F, Nugeyre MT, Chamaret S, Gruest J, Dauguet C, Axler-Blin C, Vezinet-Brun F, Rouzioux C, Rozenbaum W, Montagnier L. Science. 1983; 220:868. [PubMed: 6189183] b) Gallo RC, Salahuddin SZ, Popovic M, Shearer GM, Kaplan M, Haynes BF, Palker TJ, Redfield R, Oleske J, Safai B, et al. Science. 1984; 224:500. [PubMed: 6200936]
2. UNAIDS. AIDS Epidemic Update. 2009
3. a) Allan JS, Coligan JE, Barin F, McLane MF, Sodroski JG, Rosen CA, Haseltine WA, Lee TH, Essex M. Science. 1985; 228:1091. [PubMed: 2986290] b) Robey WG, Safai B, Oroszlan S, Arthur LO, Gonda MA, Gallo RC, Fischinger PJ. Science. 1985; 228:593. [PubMed: 2984774] c) Kowalski M, Potz J, Basiripour L, Dorfman T, Goh WC, Terwilliger E, Dayton A, Rosen C, Haseltine W, Sodroski J. Science. 1987; 237:1351. [PubMed: 3629244] d) Helseth E, Olshevsky U, Furman C, Sodroski J. J Virol. 1991; 65:2119. [PubMed: 2002555]
4. a) Klatzmann D, Champagne E, Chamaret S, Gruest J, Guetard D, Hercend T, Gluckman JC, Montagnier L. Nature. 1984; 312:767. [PubMed: 6083454] b) Dalgleish AG, Beverley PC, Clapham PR, Crawford DH, Greaves MF, Weiss RA. Nature. 1984; 312:763. [PubMed: 6096719]
5. a) Sattentau QJ, Moore JP, Vignaux F, Traincard F, Poignard P. J Virol. 1993; 67:7383. [PubMed: 7693970] b) Wu L, Gerard NP, Wyatt R, Choe H, Parolin C, Ruffing N, Borsetti A, Cardoso AA, Desjardin E, Newman W, Gerard C, Sodroski J. Nature. 1996; 384:179. [PubMed: 8906795] c) Trkola A, Dragic T, Arthos J, Binley JM, Olson WC, Allaway GP, Cheng-Mayer C, Robinson J, Maddon PJ, Moore JP. Nature. 1996; 384:184. [PubMed: 8906796] d) Choe H, Farzan M, Sun Y, Sullivan N, Rollins B, Ponath PD, Wu L, Mackay CR, LaRosa G, Newman W, Gerard N, Gerard C, Sodroski J. Cell. 1996; 85:1135. [PubMed: 8674119] e) Deng H, Liu R, Ellmeier W, Choe S, Unutmaz D, Burkhart M, Di Marzio P, Marmon S, Sutton RE, Hill CM, Davis CB, Peiper SC, Schall TJ, Littman DR, Landau NR. Nature. 1996; 381:661. [PubMed: 8649511] f) Dragic T, Litwin V, Allaway GP, Martin SR, Huang Y, Nagashima KA, Cayanan C, Maddon PJ, Koup RA, Moore JP, Paxton WA. Nature. 1996; 381:667. [PubMed: 8649512]
6. a) Chan DC, Fass D, Berger JM, Kim PS. Cell. 1997; 89:263. [PubMed: 9108481] b) Weissenhorn W, Dessen A, Harrison SC, Skehel JJ, Wiley DC. Nature. 1997; 387:426. [PubMed: 9163431]
7. Liu S, Lu H, Niu J, Xu Y, Wu S, Jiang S. J Biol Chem. 2005; 280:11259. [PubMed: 15640162]
8. a) He Y, Cheng J, Lu H, Li J, Hu J, Qi Z, Liu Z, Jiang S, Dai Q. Proc Natl Acad Sci U S A. 2008; 105:16332. [PubMed: 18852475] b) Liu S, Zhao Q, Jiang S. Peptides. 2003; 24:1303. [PubMed: 14706544] c) Liu D, Madani N, Li Y, Cao R, Choi WT, Kawatkar SP, Lim MY, Kumar S, Dong CZ, Wang J, Russell JD, Lefebure CR, An J, Wilson S, Gao YG, Pallansch LA, Sodroski JG, Huang Z. J Virol. 2007; 81:11489. [PubMed: 17686848]
9. a) Zhao Q, Ma L, Jiang S, Lu H, Liu S, He Y, Strick N, Neamati N, Debnath AK. Virology. 2005; 339:213. [PubMed: 15996703] b) Madani N, Schon A, Princiotto AM, Lalonde JM, Courter JR, Soeta T, Ng D, Wang L, Brower ET, Xiang SH, Kwon YD, Huang CC, Wyatt R, Kwong PD, Freire E, Smith AB 3rd, Sodroski J. Structure. 2008; 16:1689. [PubMed: 19000821] c) Schon A, Madani N, Klein JC, Hubicki A, Ng D, Yang X, Smith AB 3rd, Sodroski J, Freire E. Biochemistry. 2006; 45:10973. [PubMed: 16953583]
10. a) Neffe AT, Meyer B. Angew Chem Int Ed Engl. 2004; 43:2937. [PubMed: 15170309] b) Neffe AT, Bilang M, Meyer B. Org Biomol Chem. 2006; 4:3259. [PubMed: 17036114] c) Neffe AT, Bilang M, Gruneberg I, Meyer B. J Med Chem. 2007; 50:3482. [PubMed: 17602545]
11. Haim H, Si Z, Madani N, Wang L, Courter JR, Princiotto A, Kassa A, DeGrace M, McGee-Estrada K, Mefford M, Gabuzda D, Smith AB 3rd, Sodroski J. PLoS Pathog. 2009; 5:e1000360. [PubMed: 19343205]

12. a) Gopi HN, Tirupula KC, Baxter S, Ajith S, Chaiken IM. ChemMedChem. 2006; 1:54. [PubMed: 16892335] b) Cocklin S, Gopi H, Querido B, Nimmagadda M, Kuriakose S, Cicala C, Ajith S, Baxter S, Arthos J, Martin-Garcia J, Chaiken IM. J Virol. 2007; 81:3645. [PubMed: 17251295]
13. Gopi H, Umashankara M, Pirrone V, LaLonde J, Madani N, Tuzer F, Baxter S, Zentner I, Cocklin S, Jawanda N, Miller SR, Schon A, Klein JC, Freire E, Krebs FC, Smith AB, Sodroski J, Chaiken I. J Med Chem. 2008; 51:2638. [PubMed: 18402432]
14. Ferrer M, Harrison SC. J Virol. 1999; 73:5795. [PubMed: 10364331]
15. Gopi H, Cocklin S, Pirrone V, McFadden K, Tuzer F, Zentner I, Ajith S, Baxter S, Jawanda N, Krebs FC, Chaiken IM. J Mol Recognit. 2009; 22:169. [PubMed: 18498083]
16. Leavitt SA, SchOn A, Klein JC, Manjappara U, Chaiken IM, Freire E. Curr Protein Pept Sci. 2004; 5:1. [PubMed: 14965316]
17. Connor RI, Chen BK, Choe S, Landau NR. Virology. 1995; 206:935. [PubMed: 7531918]
18. Ishino T, Pillalamarri U, Panarello D, Bhattacharya M, Urbina C, Horvat S, Sarkhel S, Jameson B, Chaiken I. Biochemistry. 2006; 45:1106. [PubMed: 16430207]

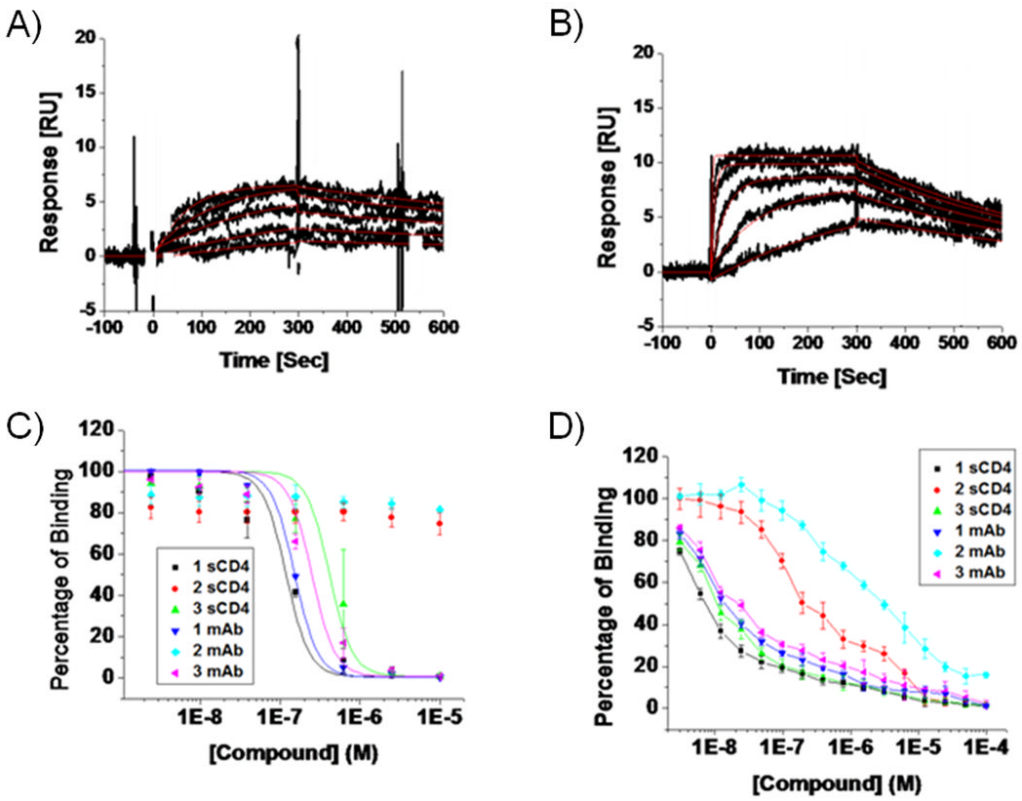

FIGURE 1.

(A & B) Direct binding of compound 2 and compound 3 (respectively) to surface-immobilized HIV-1_{YU-2} gp120. Response curves are for increasing concentrations of compound binding to immobilized HIV-1_{YU-2} gp120. Black lines indicate experimental data, whereas red lines indicate fitting to a 1:1 Langmuir binding model with a parameter included for mass transport. **(C) SPR-analyzed effects of compounds 1, 2 and 3 on the sCD4 and mAb 17b interactions with HIV-1_{YU-2} gp120.** Under the conditions of the experiment, the IC_{50} of each compound for sCD4 was determined to be 112 nM for **1** and 500 nM for **3**, while no IC_{50} value could be calculated for **2.** The IC_{50} of each compound for mAb 17b was 152 nM for **1** and 250 nM for **3** while no IC_{50} value could be calculated for **2.** **(D) Dose response curves for compounds 1, 2 and 3 determined from the effect on HIV-1_{YU-2} gp120 interaction with sCD4 and mAb 17b via ELISA.** Lines between individual data points connect the points to show the progression of data and do not represent curve fits. All data in Figure 1 were obtained from a minimum of three repeat assays.

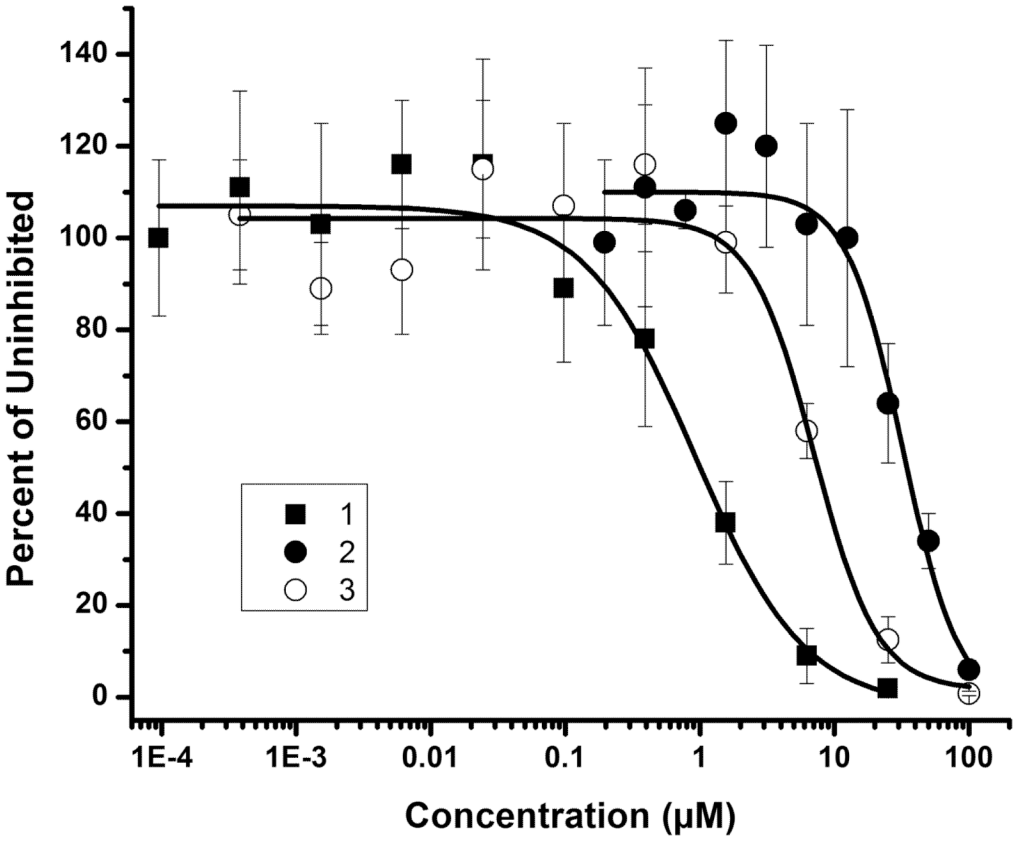

FIGURE 2. Analysis of antiviral potencies of peptides 1, 2 and 3 using single round viral infection assays

Recombinant HIV-1_{BaL} was pre-incubated with serial dilutions of **1**, **2** or **3** for 30 minutes at 37 °C. The virus-inhibitor mixture was then added to HOS.CD4.CCR5 for 48 hours. Infection was determined based on luciferase activity. Data points were fit to a simple sigmoidal inhibition model using Origin software to derive the best-fit lines. The IC_{50} values were 0.8 μM for **1**, 35 μM for **2** and 6.8 μM for **3**. Data represent a minimum of three repeats.

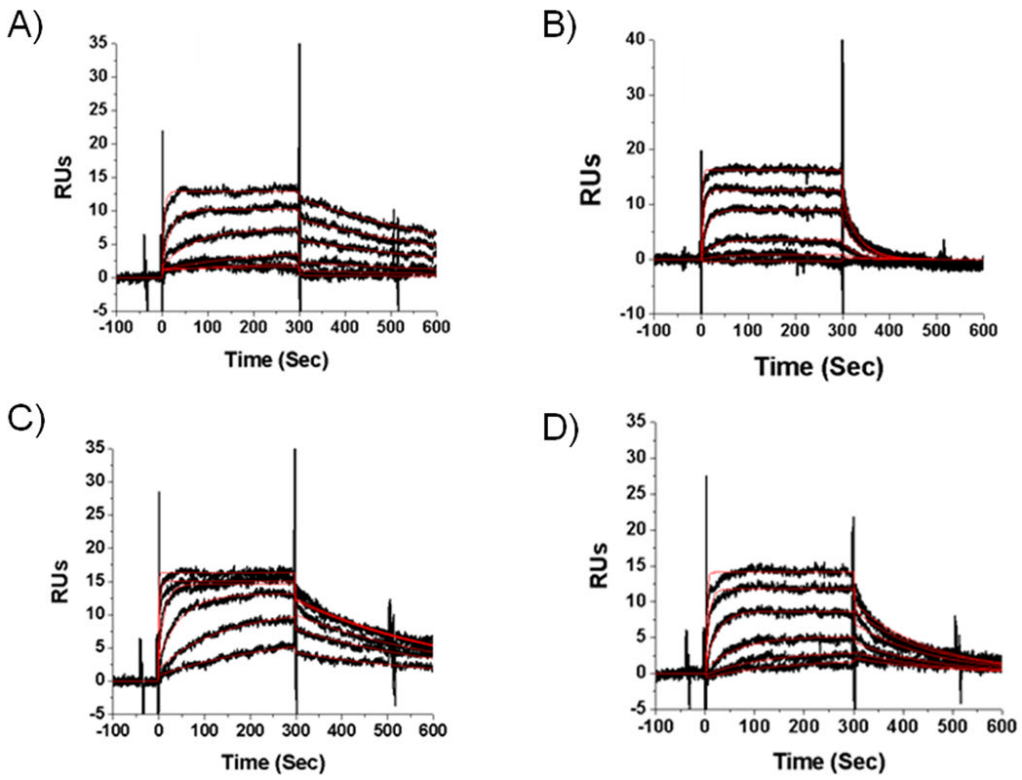

FIGURE 3. Sensograms for the direct binding of truncated peptides to immobilized HIV-1_{YU-2} gp120

(A) **1**, (B) **6**, (C) **9** and (D) **19**, each at concentrations of 2, 4, 8, 10, 50 100, 250 and 500 nM. Black lines are experimental data and red lines are fits to a 1:1 Langmuir binding model with a parameter included for mass transport.

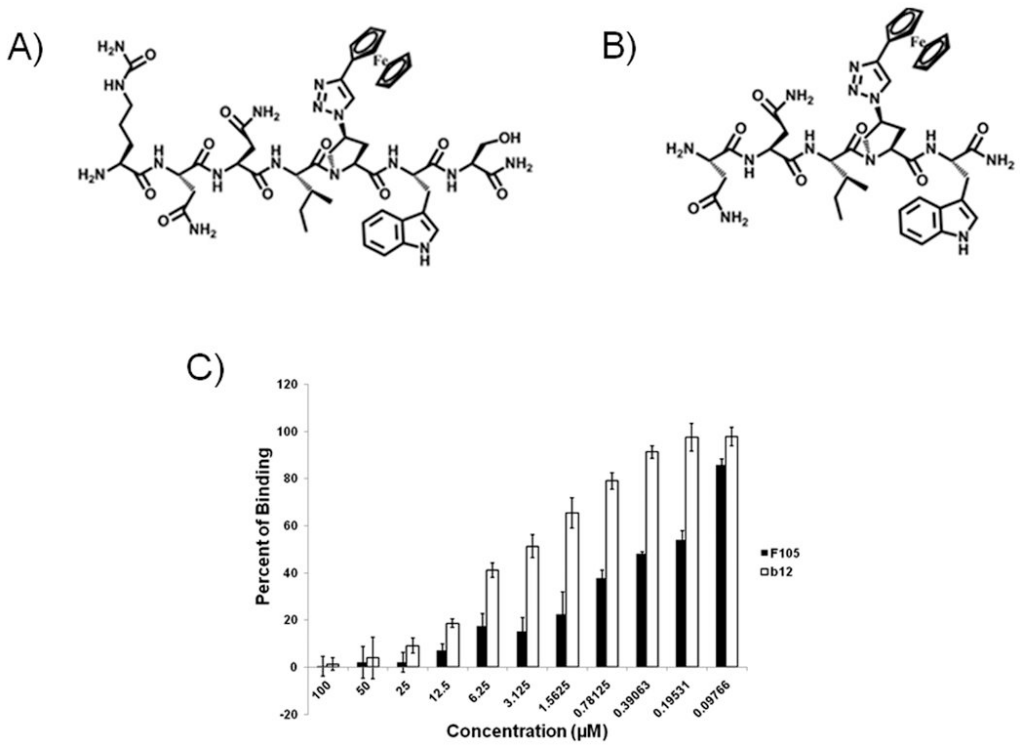

Figure 4. Structures of triazole conjugate peptides (A) 9 and (B) 19. (C) Inhibition by peptide 19 of the binding of CD4 binding site (CD4bs) antibodies to immobilized HIV-1_{YU-2} gp120

The percentage of binding of antibodies mAb F105 and IgG b12 to immobilized YU-2 gp120 is plotted against the concentration of the inhibitor peptide. Peptide **19** inhibited the binding of HIV-1_{YU-2} gp120 to F105 and b12 at IC_{50} values of 0.6 ± 0.05 and 4.0 ± 0.17 μM, respectively.

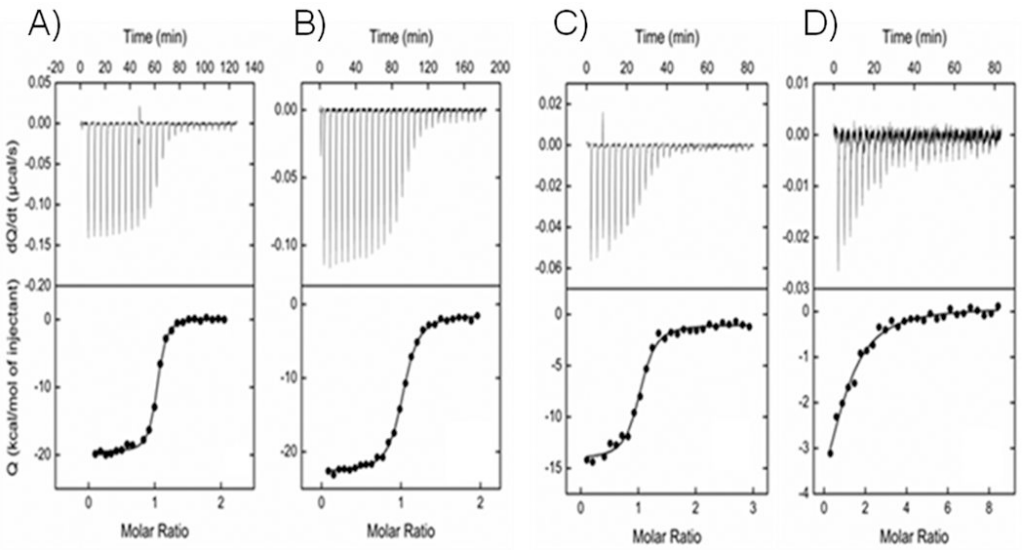

Figure 5. Calorimetric titrations of gp120 with chain-length truncated peptides

(A) **1**, (B) **9**, (C) **19** and (D) **20** at 25°C in PBS, pH 7.4. Experiments in (A) and (B) were carried out using a VP-ITC where 2 μM gp120 in the calorimetric cell (~1.4 mL) was titrated with 10 μL aliquots of peptide at concentration of 30 μM. Experiments in (C) and (D) were carried out using an ITC_{20} where 4 μM gp120 in the calorimetric cell (~200 μL) was titrated with 1.4 μL aliquots of peptides **19** and **20** at 50 and 100μM, respectively.

Table 1

Amino acid sequence and mass characterization data for truncation peptides reported in this study

Entry	Peptide Designation	Peptide Sequence	Mass (Da) Observed[a]	Mass (Da) Calculated
1	**HNG-156**	**R-I-N-N-I-X-W-S-E-A-M-M**	**1711.32**	**1711.4**
	N- and C- Terminal Truncates			
2	UM-10	X-W-S-E-A-M-M	1100.36[b]	1056.26
3	UM-12	R-I-N-N-I-X-W	1162.5	1161.53
	Side chain Variation in First Residue			
4	UM11	R-I-N-N-I-X-W-S	1249.4	1249.54
5	UM13	E-I-N-N-I-X-W-S	1235.5	1222.5
	Side chain Variation in Second Residue			
6	UM21	I-N-N-I-X-W-S	1092.41	1091.54
7	UM22	R-N-N-I-X-W-S	1137.27	1136.41
8	UM23	E-N-N-I-X-W-S	1122.53	1121.5
9	UM24	Cit-N-N-I-X-W-S	1136.6	1135.54
10	UM27	K-N-N-I-X-W-S	1107.5	1107.09
11	UM28	F-N-N-I-X-W-S	1126.5	1125.52
	Side Chain Variation in Third Residue			
12	UM31	N-N-I-X-W-S	979.4	979.38
13	UM32	R-N-I-X-W-S	1022.5	1021.43
14	UM33	E-N-I-X-W-S	994.4	994.37
15	UM34	Cit-N-I-X-W-S	1022.2	1022.42
16	UM-35	I-N-I-X-W-S	978.23	978.42
	Active Pharmacophore Sequence			
17	UM15	I-N-N-I-X-W	1005.5	1005.43
18	UM16	R-I-N-N-I-X	976.3	978.45
19	UM17	N-N-I-X-W	892.05	892.34
20	UM41	N-I-X-W-S	865.0[c]	849.76
	Stereochemistry Importance for Residue			
21	UM24-DW	Cit-N-N-I-X -W^D-S	1137.14	

[a] (M+1);

[b] (M+K) and

[c] (M+Na) peaks were observed in MALDI-TOF spectra.

ChemMedChem. Author manuscript; available in PMC 2011 November 8.

Table 2

Binding kinetics and inhibition efficacies of truncated peptides

Entry	SPR Interaction Parameters					Antiviral Activity
	K_D(nM) [a]	k_a (Ms^{-1}) [a]	k_d (S^{-1}) [a]	IC_{50} (nM) [b]		IC_{50} (μM) [c]
				sCD4	mAb 17b	
1	**6.9**	**5.5E+05** ± 0.5	**3.8E-03** ± 0.1	**112 ± 10**	**152 ± 4**	**0.8** ± 0.26
2	**809**	**1.1E+03** ± 0.6	**8.90E-04** ± 1.2	**>10,000**	**>10,000**	**35** ± 15
3	**12.9**	**1.4E+05** ± 1.3	**1.8E-03** ± 1.3	**500 ± 306**	**250 ± 39**	**6.8** ± 0.3
4	**65.6**	**3.2E+05** ± 1.8	**2.1E-02** ± 0.6			**4** ± 2.9
5	**5.5**	**5.6E+05** ± 3.2	**3.1E-03** ± 2			**1.2** ± 0.3
6	**169**	**8.3E+03** ± 5.7	**1.4E-03** ± 0.5			**7.4** ± 2.7
7	**13.3**	**5.1E+05** ± 2.1	**6.8E-03** ± 0.4			**11** ± 5
8	**26.2**	**1.3E+05** ± 0.2	**3.4E-03** ± 0.2			**5.8** ± 1.1
9	**4.1**	**7.0E+05** ± 2.8	**2.9E-03** ± 1.2	**118 ± 27**	**138 ± 11**	**2.6** ± 1.0
10	**14.9**	**5.9E+05** ± 1.4	**8.8E-03** ± 2.1			**23** ± 8.0
11	**11.3**	**3.8E+05** ± 2.1	**4.3E-03** ± 0.8			**13** ± 1.7
12	**18.6**	**4.2E+05** ± 1.5	**7.8E-03** ± 1.1	**191 ± 3**	**172 ± 16**	**16** ± 6.0
13	**939**	**3.3E+03** ± 2.7	**3.1E-03** ± 1.5			>100
14	**1636**	**1.1E+03** ± 0.9	**1.8E-03** ± 0.8			>100
15	>10000	Not Detectable	Not Detectable			>100
16	>10000	Not Detectable	Not Detectable			**17** ±7
17	**8.5**	**3.9E+05** ± 3.6	**3.3E-03** ± 0.3	**236 ± 17**	**238 ± 4**	**6.9** ± 0.8
18	>10000	Not Detectable	Not Detectable			>100
19	**333**	**1.8E+04** ± 0.67	**6.0E-03** ± 1.25	**147 ± 6**	**241 ± 63**	**33** ± 11
20	>10000	Not Detectable	Not Detectable			>200
21	>10000	Not Detectable	Not Detectable	**>10,000**	**>10,000**	>100

[a] Kinetics values were determined using SPR by direct binding of compound to immobilized HIV-1_{YU-2} gp120. Data were fit to a 1:1 Langmuir binding model with a parameter included for mass transport.

[b] SPR IC_{50} values were determined using competition SPR.

[c] Antiviral IC_{50} values were obtained through a single round infection assay and expressed as relative infection versus untreated (100%). All data represent a minimum of three experiments.

Table 3
Binding thermodynamics of truncated peptides to gp120[a]

Peptide	K_D (nM)	ΔG (kcal mol^{-1})	ΔH (kcal mol^{-1})	$-T\Delta S$ (kcal mol^{-1})
1	7.8	−11.1	−19.9	+ 8.8
3	65	−9.8	−19.7	+9.9
9	25	−10.4	−16.7	+6.3
12	80	−9.7	−13.8	+4.1
17	45.5	−10.0	−16.6	+6.6
19	69	−9.8	−13.2	+3.3
20	2300	−7.7	−6.1	−1.6

[a] Isothermal titration calorimetric experiments were performed at 25 °C in1× PBS (pH 7.4).